

Local and non-local equivalent potentials for p - ^{12}C scattering

A. Lovell and K. Amos
*School of Physics, University of Melbourne,
Victoria 3052, Australia.*

Abstract

A Newton-Sabatier fixed energy inversion scheme has been used to equate inherently non-local p - ^{12}C potentials at a variety of energies to pion threshold, with exactly phase equivalent local ones. Those energy dependent local potentials then have been recast in the form of non-local Frahn-Lemmer interactions.

arXiv:nucl-th/0007031v1 14 Jul 2000

I. INTRODUCTION

Over the years, local nuclear optical potentials have been used predominantly as the interaction potentials between colliding nuclei. Frequently, those local interactions were specified phenomenologically as Woods-Saxon (WS) optical potentials; the parameter values of which were determined by variation to find best fits to nuclear elastic scattering data. The geometries of those WS forms often were taken commensurate with known attributes of nuclear densities and/or to be consistent with the character of Hartree fields for the nuclei. Most importantly in many cases, quality fits to scattering data were obtained using these local potential forms, with parameter values that varied smoothly with energy and mass. In reality however, as the optical potentials can be specified in many nucleon scattering theory as a folding of pairwise nucleon-nucleon NN interactions with nuclear structure, they must be non-local. That is assured by the Pauli principle which implies that the scattering theory involves nucleon exchange amplitudes.

For nucleon-nucleus (NA) elastic scattering, it is now possible to define non-local optical potentials in coordinate space and to use them without recourse to localization techniques [1]. Solutions of the attendant integro-differential forms of the Schrödinger equations with those non-local NA potentials have given good to excellent fits to cross-section and analyzing power data for a wide range of target masses and for energies 40 to 800 MeV [1-3]. Those non-local NA potentials are formed by folding effective, medium dependent, two-nucleon (NN) interactions with the one body density matrices (OBDME) of the target nucleus. Very good results for light mass nuclei in particular have been obtained when those OBDME were specified from shell model (or similar) calculations involving very large and complete shell spaces.

Nevertheless, for a multitude of uses, such as with application of multi-step reaction theories and scattering into the continuum, it is useful to define a local form of optical potential for the pA scattering system. Note also that equivalent local potentials can be used to account for the coupled channels effects in scattering [4], the resulting form related to that found by localization of exchange amplitudes. There are many ways in which a local potential can be specified and considered equivalent to a non-local one. Some have been reviewed recently [1]. Herein we consider a form that is to be phase equivalent. The phase shifts provided by the g -folding (non-local) potentials used recently [3] to find very good predictions of p - ^{12}C elastic scattering, have been used as input to finding solutions of fixed energy quantum inverse scattering theory. In particular we have found the equivalent local potentials by using a modified version of the Newton-Sabatier inversion scheme that has been proposed by Lun *et al.* [5]. This method allows extraction of both central and spin-orbit interactions from the input phase shift values. It is not the only fixed energy method that can do so. Hooshyar [6] has used the Sabatier interpolation formulae in a finite difference inversion method, and Huber and Leeb [7] have investigated an approach to this problem based upon Darboux transformations. Likewise an approximate scheme [8] has been used with some success [9] to analyze neutron-alpha particle scattering data in particular. However, the scheme we adopt is most facile, reducing the process of inversion to finding solution of a system of linear-algebraic equations.

Fixed energy inverse scattering schemes are not the only ways to effect the transition from non-local potentials to equivalent local ones and *vice versa*. Various other approxi-

mations and analytic expressions exist [1]. However, all such other methods rely upon the range of the non-locality being small in comparison to the size of most nuclei. If such is also the case with regard to the de Broglie wavelength of the projectile, a semi-classical WKB approximation may be valid. However, Peierls and Vinh-Mau [10] note that while the localization approximations should be well met within the medium of a large nucleus, corrections could be important in the nuclear surface region and for light mass nuclei. In any circumstance that the non-locality range exceeds the characteristic length of the system, they note that the non-local potential cannot be approximated by their algorithm of localization. A desirable feature of using inverse scattering theory to define equivalent local potentials is that none of these approximations are invoked. But such must be borne in mind when the reverse process, of defining a utilitarian non-local form from the energy variation of a set of local potentials, is considered. In doing that reverse process, we chose a mapping used by Apagyi *et al.* [11] for its simplicity and as the data sets we study exist at disparate energies in the range 65 to 250 MeV.

In this paper the salient features of the modified Newton-Sabatier fixed energy inversion scheme are discussed first. Then in Sec. III, we present and discuss the results of this non-local to phase equivalent local potential scheme. The method to recast non-local forms from energy variation of local potentials is then defined in Sec. IV, and results of mapping the local optical potentials back to non-local interaction forms of Frahn-Lemmer type [12] are given then in Sec. V. Conclusions are drawn in Sec. VI.

II. THE MODIFIED NEWTON-SABATIER FIXED ENERGY INVERSION SCHEME

The modified Newton-Sabatier method [5] permits extraction from a set of scattering phase shifts, not only of a central local interaction between two colliding quantum objects but also a spin-orbit term. The approach relies on analogues of the Regge-Newton equations for interactions involving the spin-orbit component of the potential, namely the Sabatier transformation equations [13]. In this method, the non-linear Sabatier interpolation formulae essentially are converted into a finite set of linear-algebraic equations which are easily solved.

With most inverse scattering theories, the assumed equation of motion is the homogeneous Schrödinger equation, the radial terms of which we consider in the form

$$\left[\frac{d^2}{dr^2} + \frac{2\mu E}{\hbar^2} - \frac{\ell(\ell+1)}{r^2} - \frac{2\mu}{\hbar^2} V(r) \right] R_{\ell,s,j}(r) = 0. \quad (1)$$

$V(r)$ is the hadronic interaction potential which we assume is a sum of central and spin-orbit terms, viz.

$$V(r) = [V_c(r) + V_{so}(r) \boldsymbol{\ell} \cdot \boldsymbol{\sigma}], \quad (2)$$

where $\boldsymbol{\sigma} = 2\mathbf{s}$. With charged particle scattering, $V_c(r)$ also includes the Coulomb potential.

Since the energy is fixed it is convenient to recast Eq. (1) into a dimensionless form, using the following notation

$$\rho = kr, \quad k^2 = \frac{2\mu E}{\hbar^2}, \quad U_c(\rho) = \frac{V_c(r)}{E} \quad \text{and} \quad U_{so} = \frac{V_{so}}{E}. \quad (3)$$

The dimensionless, decoupled, reduced radial Schrödinger equations subsequently are

$$\left[\frac{d^2}{d\rho^2} + 1 - U_c(\rho) + sU_{so}(\rho) \mp 2s\lambda U_{so}(\rho) - \frac{\lambda^2 - \frac{1}{4}}{\rho^2} \right] \chi_\lambda^\pm(\rho) = 0 \quad (4)$$

where $\lambda (= \ell + \frac{1}{2})$ is the angular momentum variable.

As two unknowns, $V_c(r)$ and $V_{so}(r)$, are sought, only two of the $(2s+1)$ possible equations in Eq. (4) are required. It is convenient to choose the cases for which $j = \ell \pm s$ associated with which are two sets of phase shifts denoted by δ_ℓ^+ and δ_ℓ^- respectively. This method can be used with particles of any spin. For NA scattering, the nucleon intrinsic spin of course is $\frac{1}{2}$, but we must presume that the spin of the nucleus is not an influential factor in scattering, i.e. we equate all such scattering to that from a spin zero target so that the quantum number is $j = \ell \pm \frac{1}{2}$. This is precisely the case though for $p\text{-}^{12}\text{C}$ scattering that we investigate herein. The superscripts ‘ \pm ’ now designate the relevant two values of j .

The Sabatier interpolation formulae relate the regular solutions of Eq. (4), $\chi_\lambda^\pm(\rho)$, to the set $\{\psi_\lambda(r)\}$, which are solutions of the Schrödinger equations for a reference potential, $U_0(r)$, that are regular at the origin. The link is

$$\chi_\lambda^\pm(\rho) = F^\pm(\rho)\psi_\lambda(\rho) + \sum_{\mu \in \Omega} \frac{2\mu}{\pi} W_{\lambda\mu}(\rho) [b_\mu \chi_\mu^\pm(\rho) - a_\mu^\pm \chi_\mu^\mp(\rho)] \quad (5)$$

where

$$W_{\lambda\mu}(\rho) = \frac{\psi_\mu(\rho)\psi'_\lambda(\rho) - \psi_\lambda(\rho)\psi'_\mu(\rho)}{\lambda^2 - \mu^2} \quad (6)$$

is the Wronskian. The set of scalar functions, F^\pm , in Eq. (5) are defined by

$$\begin{aligned} F^\pm(\rho) &= \exp \left[\pm \int_0^\rho t S U_s(t) dt \right] \\ &= \frac{2}{\pi\rho} a_0 \chi_0(\rho) \psi_0(\rho) + \frac{2}{\pi\rho} \sum_{\mu \in S} [a_\mu^\pm \chi_\mu^\mp(\rho) + b_\mu \chi_\mu^\pm(\rho)] \psi_\mu(\rho) \end{aligned} \quad (7)$$

and obey the following property:

$$F^+(\rho)F^-(\rho) = 1. \quad (8)$$

Solution of these equations rely on a complete knowledge of all the phase shifts, δ_λ^\pm , where $\lambda \equiv \ell + 0.5$ now includes not only the set of corresponding to the physical set of integer ℓ but also all half-integer values. As such, the summations span the set of angular momenta $\Omega : \{\frac{1}{2}, 1, \frac{3}{2}, 2, \frac{5}{2}, 3, \dots\}$. Naturally, analysis of scattering data can provide only the physical set of phase shifts, i.e. those corresponding to integer ℓ . Interpolation of the (physical) data set is then required to define the required set for inversion. Of course if instead one wishes to map against a defined non-local potential, then the phase shifts at the intervening values for λ can be evaluated.

Eqs. (5) and (7) contain a set of unknown coefficients a_λ^\pm . Eq. (7) also includes functions $\chi_0(\rho)$ and $\psi_0(\rho)$ which are solutions of the relevant Schrödinger equations for $\ell = -\frac{1}{2}$. In addition there are the weights b_λ which are defined [14] by

$$b_\lambda = \frac{\gamma(\lambda + \frac{1}{2} - i\eta)\gamma(\lambda + \frac{1}{2} + i\eta)}{[\gamma(\lambda + \frac{1}{2})]^2} \begin{cases} \cosh(\pi\eta) & \text{integer } \lambda \\ -\sinh(\pi\eta) & \text{half - integer } \lambda \end{cases} . \quad (9)$$

The set of equations, Eqs. (5) and (7), constitute a matrix problem to specify the unknown coefficients, a_λ^\pm , and the functions, F^\pm , when select large radial values ρ_i are chosen so that

$$\begin{aligned} \psi_\lambda^\pm(\rho_i) &= \sin \left[\rho_i - \frac{1}{2} \left(\lambda - \frac{\pi}{2} \right) + \sigma_\lambda - \eta \ln(2\rho_i) \right] \\ \chi_\lambda^\pm(\rho_i) &= c_\lambda^\pm \sin \left[\rho_i - \frac{1}{2} \left(\lambda - \frac{\pi}{2} \right) + \delta_\lambda^\pm - \eta \ln(2\rho_i) \right] \\ F^\pm(\rho_i) &= h^\pm; \quad (\text{constants}) , \end{aligned} \quad (10)$$

where σ_λ are the Coulomb phase shifts and c_λ^\pm are additional unknown constants to be determined. Taking two (or more) distinct radial values, $(\rho_i = \rho_1, \rho_2, \dots \geq \rho_0)$, and with $\chi_\lambda^\pm(\rho) \equiv c_\lambda^\pm T_\lambda^\pm(\rho)$, Eqs. (5) and (7) can be recast as

$$\psi_\lambda(\rho_i) = C_\lambda^\pm T_\lambda^\pm(\rho_i) + \sum_{\mu \in S'} \frac{2\mu}{\pi} W_{\lambda\mu}(\rho_i) \left[T_\mu^\mp(\rho_i) A_\mu^\pm - b_\mu T_\mu^\pm(\rho_i) C_\mu^\pm \right] . \quad (11)$$

They form a set of linear equations in the unknown coefficients which have been grouped as

$$A_\lambda^\pm = a_\lambda^\pm c_\lambda^\mp h^\mp \quad \text{and} \quad C_\lambda^\pm = c_\lambda^\pm h^\mp . \quad (12)$$

The set S' is limited to λ_{max} so that the matrix is finite and we can find a solution by using singular value decomposition (SVD); a useful approach since the matrix may tend to be ill-conditioned. By so doing we presume that from a characteristic radius, $\rho_0 = kr_0$, the interaction is solely Coulombic (or zero for incident neutrons) and that for all $\lambda > \lambda_{max}(\rho_0)$, $\delta_\lambda^\pm - \sigma_\lambda \rightarrow 0$. With the coefficients a_λ^\pm , and c_λ^\pm defined (h^\pm are specified in terms of them), multiplication of Eq. (5) by $F^+(\rho)$ and upon rearrangement, gives a set of $(8 * \lambda_{max} + 1)$ linear equations,

$$\begin{aligned} [F^+(\rho)]^2 \psi_\lambda(\rho) &= F^+(\rho) \chi_\lambda^+(\rho) - \sum_{\mu \in \Omega'} \frac{2\mu}{\pi} W_{\lambda\mu}(\rho) \left[b_\mu F^+(\rho) \chi_\mu^+(\rho) - a_\mu^+ F^+(\rho) \chi_\mu^-(\rho) \right] \\ \psi_\lambda(\rho) &= F^+(\rho) \chi_\lambda^-(\rho) - \sum_{\mu \in \Omega'} \frac{2\mu}{\pi} W_{\lambda\mu}(\rho) \left[b_\mu F^+(\rho) \chi_\mu^-(\rho) - a_\mu^- F^+(\rho) \chi_\mu^+(\rho) \right] \\ [1 - (F^+(\rho))^2] \psi_0(\rho) &= \sum_{\mu \in \Omega'} \frac{2\mu}{\pi} W_{0\mu}(\rho) \left[(b_\mu + a_\mu^-) F^+(\rho) \chi_\mu^+(\rho) - (b_\mu + a_\mu^+) F^+(\rho) \chi_\mu^-(\rho) \right] , \end{aligned} \quad (13)$$

that can be solved for the $(8 * \lambda_{max} + 1)$ values of $F^+(\rho) \chi_\lambda^\pm(\rho)$ and $F^+(\rho)$ at each value of $\rho \leq \rho_0$ desired. Then, as Chadan and Sabatier [14] have shown, the inversion potentials are obtained from identities

$$\begin{aligned} U_{so}(\rho) &= \pm \frac{2}{\rho} \frac{d \ln(F^\pm(\rho))}{d\rho} \quad \text{with} \quad F^+(\rho) F^-(\rho) = 1 \\ U_c(\rho) &= U_0(\rho) + \frac{1}{2} U_{so}(\rho) - \frac{1}{\rho} \frac{d}{d\rho} [G^+(\rho) F^-(\rho) + G^-(\rho) F^+(\rho)] + \frac{1}{4} [\rho U_{so}(\rho)]^2 , \end{aligned} \quad (14)$$

where

$$G^\pm(\rho) = \frac{2}{\pi\rho} \sum_{\mu \in \Omega} \mu \left[a_\mu^\pm \chi_\mu^\mp(\rho) - b_\mu \chi_\mu^\pm(\rho) \right] \psi_\mu(\rho) . \quad (15)$$

Inherent with inversion potentials from all Newton-Sabatier methods is a pole at the origin. That pole arises from the s-wave contributions in the summations [15] but it usually influences only small radii properties of the results. In most cases studied, the effects of the pole are not evident beyond 0.5 fm typically.

The Coulomb field poses a problem with inverse scattering theory applications. The scattering phase shifts with a Coulomb potential incorporated increase with ℓ . However, a transformation of phase shifts allows that problem to be allayed [16]. At and beyond a radius r_0 , the nuclear component in the total potential can be ignored. So at r_0 the Schrödinger potential is given by $V_c(r_0) = 2\eta E/\rho_0$. The method is to take that value for a new potential at all larger radii, and hence that new potential is

$$\tilde{V}(r) = \begin{cases} V(r) & r < r_0 = \rho_0/k \\ V_c(r_0) & r \geq r_0 \end{cases} . \quad (16)$$

For this potential, the internal solutions are then to be matched to Bessel functions (zero reference potential solutions). Subtracting the long ranged constant potential $V_c(r_0)$ from the overall one,

$$\tilde{V}(r) - V_c(r_0) = \begin{cases} V_c(r) - V_c(r_0) & r < r_0 \\ 0 & r > r_0 \end{cases} , \quad (17)$$

gives a new potential which when used in the Schrödinger equation gives rise to a new but essentially equivalent set of phase shifts. By matching the logarithmic derivatives at r_0 with the external, zero potential solutions, one finds the relation

$$\frac{d}{dr} \log[\cos \tilde{\delta}_\lambda H_\lambda(\beta\rho_0) + \sin \tilde{\delta}_\lambda I_\lambda(\beta\rho_0)] = \frac{d}{dr} \log[\cos \delta_\lambda \psi_\lambda(\beta\rho_0) + \sin \delta_\lambda \zeta_\lambda(\beta\rho_0)] , \quad (18)$$

where H_λ and I_λ are the regular and irregular zero potential solutions respectively and $\beta = \sqrt{1 - V(\rho_0)/E_{cm}}$ ($= \sqrt{1 - 2\eta/\rho_0}$ for a Coulomb potential). The new phase shifts are then given by

$$\tilde{\delta}_\lambda = - \arctan \left(\frac{H'_\lambda(\beta\rho_0) - H_\lambda(\beta\rho_0)D_\lambda}{I'_\lambda(\beta\rho_0) - I_\lambda(\beta\rho_0)D_\lambda} \right) \quad (19)$$

where

$$D_\lambda(\rho_0) = i \left[\frac{\cos \delta_\lambda \psi'_\lambda(\rho_0) + \sin \delta_\lambda \zeta'_\lambda(\rho_0)}{\cos \delta_\lambda \psi_\lambda(\rho_0) + \sin \delta_\lambda \zeta_\lambda(\rho_0)} \beta \right] . \quad (20)$$

Thus inversion is made of these new phase shifts with a zero reference potential to obtain $\tilde{U}(\rho)$ from which and on accounting for the energy shift, the actual potential for $r < r_0$ is

$$V(r) = E \left[\beta^2 \tilde{U}(r) + 1 - \beta^2 \right] , \quad r = \frac{\rho}{k\beta} \quad (21)$$

III. RESULTS AND DISCUSSION

Using medium modified effective NN interactions between a projectile proton and each and every bound nucleon in ^{12}C , microscopic non-local complex and spin dependent optical potentials have been generated for a range of energies, 40 to 800 MeV in fact [3]. The resulting cross sections and analyzing powers so predicted are in good agreement with the observed data. Those calculations were made using the program DWBA98 [17]. Therein, at each (fixed) energy, the appropriate effective NN interaction is folded with the OBDME of the target. For ^{12}C those OBDME were generated from complete $(0+2)\hbar\omega$ space shell model wave functions [2]. That program also solves the integro-differential form of Schrödinger equations, and thereby we obtained sets of phase shifts of (non-local) optical potentials to use as input to the inversion procedure.

A. The equivalent local potentials from inversion

The inversion potentials obtained using the g -folding model phase shift sets specified for proton scattering from ^{12}C with energies 65, 100, 160, 200, and 250 MeV are displayed in Fig. 1 by the solid, dashed, long dashed, dotted and dot-dashed curves respectively. Results have been found for 135 MeV protons as well and they are intermediary to those shown. In segments (a) and (b) the real and imaginary parts of the central potentials are displayed while segments (c) and (d) respectively contain the real and imaginary components of the spin-orbit potentials. The central potential values progressively becoming less refractive and more absorptive with increasing energy. The spin-orbit potentials have more variation in their structure with energy although there is a general shape for the real and imaginary components.

Clearly while these components of the inversion potentials vary smoothly with energy, the central terms especially, their shape is not characteristic of traditional potentials, e.g. a Woods-Saxon function and/or its derivative. That is so independent of the inherent pole term in the inversion method which dominates the inversion potential values at the origin. But, as noted previously [15], that pole influence is minimal beyond about 0.5 fm. Also at each energy, the effect of the pole when the inversion potential was used in calculation of scattering observables was small if not negligible. Of primary interest then is the behavior of the inversion potentials from approximately 1 fm and our comments pertain to the properties from that radius out.

In Fig. 1, the real components of the central potentials found by inversion are shown in panel (a). At 65 MeV this component varies almost linearly between 1 and 4 fm in radius before tapering to zero, and then rather slowly. With increasing energy some structure develops in the central real potential for radii $1 < r < 4$ fm eventually, at 250 MeV, becoming a shoulder shaped well. While values of the real central potential in that region ($1 < r < 4$ fm) decrease in strength to form the shoulder shape, the longer range property increases in effect with energy.

There is a different trend in the imaginary components of the central inversion potentials as is evident in segment (b) of Fig. 1. At all energies the long ranged character of the central imaginary interactions ($r > 3.5$ fm) is the same and the component rapidly vanishes with large r , contrasting markedly with the properties of the associated central real terms. With

increasing energy the central absorption also increases markedly in the body of the nucleus ($1 < r < 3.5$ fm in this case) with a noticeable structure in the 65 MeV potential result. That absorptive character however is almost linear at 250 MeV.

The real and imaginary components of the spin-orbit potentials found by inversion are shown in segments (c) and (d) of Fig. 1. They are relatively weak, the imaginary parts especially so save for the result at 65 MeV. Overall these potentials are very similar; the real parts having a weak attractive well (about 2.5 MeV deep at $r \sim 1.8$ fm) with a shorter ranged repulsion. No serious import should be attached as yet to the specifics of the structures shown, other than that they are the result of using the particular input set of phase shifts. Possible adjustments to the basic NN effective interactions in the original non-local potential generation could vary what we are to use as input phase shifts sufficiently to alter the small magnitude details of the spin-orbit components shown here.

B. The Phase Shifts

Two potentials may be considered equivalent if they give the same scattering phase shifts. In principle the inversion potentials will be so. Nevertheless, the inversion potentials must be used to get ‘inversion’ phase shifts for comparison against the original values to check that they are indeed equivalent. In Fig. 2 these sets are compared for all energies. The real and imaginary parts of the phase shifts values are shown in the left and right panels respectively while those for $j = \ell + 0.5$ and for $j = \ell - 0.5$ are given in the top and bottom sections respectively. The input phase shift values are depicted by the filled circles while the results found from the inversion potentials are indicated by the connecting lines. The notation with energy is that used in Fig. 1. Clearly there is excellent agreement between the phase shifts found from the local, inversion potentials and from the g -folding non-local ones.

There is a relatively smooth and consistent change in the phase shift values as the energy increases. The real parts of the sets corresponding to $j = \ell + 0.5$ and $j = \ell - 0.5$ both show a steady decrease in value with energy for small partial waves, while the associated imaginary parts show a steady increase. The notable exception is the 65 MeV case for which the imaginary parts differ from this pattern. In the case of the imaginary parts of the $j = \ell + 0.5$ phase shifts there is an unusual structure in the 65 MeV data set for the values $\ell < 5$.

A closer inspection of the results revealed that the s-wave phase shifts are slightly different from the original input values in both the 65 MeV and the 100 MeV cases. This variation, however, is less than four percent. The fact that the phase shifts corresponding to $\ell = 0$ differ is not unusual since the centrifugal barrier screens all other partial wave solutions from any (small) effect of the pole terms inherent in the inversion potentials.

C. The cross sections and analyzing powers

Although the excellent agreement between phase shift sets obtained from the local (inversion) and from original non-local (full folding optical) potentials for the p-¹²C scattering at diverse energies is convincing, another way to demonstrate this equivalence is to compare

the associated observables. By so doing any small variation in phase shifts that may exist can be emphasized. This is so as the cross section spans several orders of magnitude and then small inaccuracies within the phase shifts could be very apparent at the larger scattering angles particularly. The analyzing power likewise should be sensitive to small differences in the phase shift values since that observable is given by differences between scattering probabilities and is normalized by the differential cross-section values.

The cross sections and analyzing powers at the set of energies chosen (65 to 250 MeV) are given in Fig. 3. In the top section of Fig. 3, the cross sections for each energy are displayed. Once again the values of the the cross sections obtained from the full microscopic NN folding non-local potentials are represented by the circles and squares and the results obtained by using the inversion potentials are portrayed by the diverse lines. The coding of those lines for each energy is as used in Fig. 1. Circles and squares, filled and open, have been used to display the ‘data’ to differentiate the set for each energy. These cross section results demonstrate that the inversion potentials are very good local equivalents. The cross section reproductions span eight orders of magnitude and only for magnitudes less than 10^{-2} mb/sr are small divergences evident. Such divergence is most evident with the 200 MeV and 250 MeV cases since those cross sections decrease most rapidly.

An even finer test of the agreement based upon observables between the local and non-local potentials are the results for the analyzing powers. As shown in the bottom section of Fig. 3, reproduction of the analyzing power for each energy is very good out to a center of mass scattering angle of 60° . Even then only the cases of 65 and 100 MeV have any noticeable divergence between the local and non-local potentials results. It is surmised that the small variations in the values of low- ℓ phase shifts are the cause as such variations little effect predictions for the cross sections. We conjecture that this behavior is a result of the choice we have made for the phase shift value at the (unphysical) angular momentum, $\ell = -0.5$; a quantity required in the inversion process.

IV. FRAHN-LEMMER FORMS FROM LOCAL ENERGY DEPENDENT POTENTIALS

The problem is to use local forms of complex potential $V_{\text{LEQ}}(\mathbf{r}; E) = V(\mathbf{r}; E)$ which when used in the Schrödinger equation,

$$\frac{\hbar^2}{2\mu} \nabla^2 \phi(\mathbf{k}, \mathbf{r}) + [E - V(\mathbf{r}; E)] \phi(\mathbf{k}, \mathbf{r}) = 0, \quad (22)$$

give phase shifts equal to those found by solution of the non-local equations,

$$\frac{\hbar^2}{2\mu} \nabla^2 \chi^{(+)}(\mathbf{k}, \mathbf{r}) + E \chi^{(+)}(\mathbf{k}, \mathbf{r}) - \int U(\mathbf{r}, \mathbf{r}'; E) \chi^{(+)}(\mathbf{k}, \mathbf{r}') d\mathbf{r}' = 0, \quad (23)$$

where that non-local form is of the Frahn-Lemmer type [12].

If the range of non-locality in $U(\mathbf{r}, \mathbf{r}'; E)$ is small, then to evaluate the integral term in the general form, Eq. 23, of the Schrödinger equation, it is not necessary to know the solution function $\chi^{(+)}(\mathbf{k}, \mathbf{r})$ at all positions. One only needs to know how $\chi^{(+)}(\mathbf{k}, \mathbf{r})$ varies in a volume element characterized by a small distance ‘ \mathbf{s} ’ about the point ‘ \mathbf{r} ’. In that volume

element, $\chi^{(+)}(\mathbf{k}, \mathbf{r})$ oscillates with a wave number $\mathbf{K}(\mathbf{r})$ so that integration over ‘ \mathbf{s} ’ will select only those momentum components of any kernel that are in the neighborhood of $\mathbf{K}(\mathbf{r})$. This justifies expansion of the Fourier transform of a kernel $G(\mathbf{s})$ about the local wave number,

$$G(\mathbf{s}) = \frac{1}{(2\pi)^3} \int \tilde{G}(p) e^{-i\mathbf{p}\cdot\mathbf{s}} d\mathbf{p} , \quad (24)$$

and retention of only the first two terms in the expansion,

$$\tilde{G}(p) = \tilde{G}(p^2) = \tilde{G}(K^2) + (p^2 - K^2) \frac{d}{d(K^2)} \tilde{G}(K^2) + \dots . \quad (25)$$

In a simple manner then a local equivalent potential to the exchange term in Eq. (23) can be obtained by a Taylor series expansion,

$$\begin{aligned} \int U(\mathbf{r}, \mathbf{r}'; \mathbf{E}) \chi^{(+)}(\mathbf{k}, \mathbf{r}') d\mathbf{r}' &\approx \int U(\mathbf{r}, \mathbf{r}'; \mathbf{E}) e^{i(\mathbf{r}'-\mathbf{r})\cdot\nabla} \chi^{(+)}(\mathbf{k}, \mathbf{r}) d\mathbf{r}' \\ &= \left[\int U(\mathbf{r}, \mathbf{r}'; \mathbf{E}) e^{i(\mathbf{r}'-\mathbf{r})\cdot\kappa} d\mathbf{r}' \right] \chi^{(+)}(\mathbf{k}, \mathbf{r}) \end{aligned} \quad (26)$$

where a local wave number,

$$\kappa(r) = \sqrt{2\mu [E - V(r; E)]} , \quad (27)$$

has replaced the gradient operator.

Frahn and Lemmer [12] assumed that the non-local kernels of the full Schrödinger equation, Eq. (23), have a separable form (this is also known in the literature as the Perey-Buck prescription),

$$U(\mathbf{r}, \mathbf{r}'; E) \rightarrow F(\mathbf{R}) v(\boldsymbol{\rho}) , \quad (28)$$

where

$$\mathbf{R} = \frac{1}{2}(\mathbf{r} + \mathbf{r}') \quad ; \quad \boldsymbol{\rho} = \mathbf{r} - \mathbf{r}' . \quad (29)$$

Furthermore, they assume that $F(\mathbf{R}) = F(R)$ with $F(R)$ a slowly varying function about $R = r$, and that

$$v(\boldsymbol{\rho}) = v(\rho) = (\pi\sigma^2)^{-\frac{3}{2}} \exp\left(-\frac{\rho^2}{\sigma^2}\right) , \quad (30)$$

where σ is the non-locality range. A Taylor expansion about ‘ \mathbf{r} ’ gives to second order

$$\begin{aligned} F(R) \chi^{(+)}(\mathbf{k}, \mathbf{r}') &\approx \\ &F(r) \chi^{(+)}(\mathbf{k}, \mathbf{r}) + \frac{1}{6} \rho^2 \left\{ \frac{d}{dr} F(r) \frac{d}{dr} + F(r) \nabla^2 + \frac{1}{4r} \frac{d^2}{dr^2} [rF(r)] \right\} \chi^{(+)}(\mathbf{k}, \mathbf{r}) \end{aligned} \quad (31)$$

and this gives

$$\int U(\mathbf{r}, \mathbf{r}'; E) \chi^{(+)}(\mathbf{k}, \mathbf{r}') d\mathbf{r}' \approx \left\{ v_0 F(r) + \frac{1}{8} v_2 \frac{1}{r} \frac{d^2}{dr^2} [rF(r)] + \frac{1}{2} v_2 \frac{d}{dr} F(r) \frac{d}{dr} + \frac{1}{2} v_2 F(r) \right\} \chi^{(+)}(\mathbf{k}, \mathbf{r}), \quad (32)$$

where v_n are the moments of the non-locality,

$$v_n = \frac{4\pi}{(2n-1)} \int_0^\infty v(\rho) \rho^{(2+n)} d\rho. \quad (33)$$

Under this approximation, the non-local Schrödinger equation reduces to

$$\left\{ \left[-\frac{\hbar^2}{2\mu} + \frac{1}{4} \sigma^2 F(r) \right] \nabla^2 + \frac{1}{4} \sigma^2 \frac{d}{dr} F(r) \frac{d}{dr} - E + F(r) + \sigma^2 \frac{1}{r} \frac{d^2}{dr^2} [rF(r)] \right\} \chi^{(+)}(\mathbf{k}, \mathbf{r}) = 0, \quad (34)$$

which maps to an equivalent local and energy dependent form,

$$\left[-\frac{\hbar^2}{2\mu} \nabla^2 + V(r, E) - E \right] \varphi(\mathbf{k}, \mathbf{r}) = 0, \quad (35)$$

upon using a point transformation defined by

$$\varphi(\mathbf{k}, \mathbf{r}) = T(r) \chi^{(+)}(\mathbf{k}, \mathbf{r}). \quad (36)$$

Multiplication of Eq. (34) by $T(r)$ gives

$$T(r) \left\{ -\frac{\hbar^2}{2\mu} \nabla^2 - \left[\frac{J_1(r)}{X(r)} \right] \frac{d}{dr} \left[\frac{J_0(r) + E}{X(r)} \right] \right\} T^{-1}(r) \varphi(\mathbf{k}, \mathbf{r}) = 0, \quad (37)$$

with the functions,

$$\begin{aligned} J_0(r) &= F(r) + \frac{\sigma^2}{16r} \frac{d^2}{dr^2} [rF(r)], \\ J_1(r) &= \frac{\sigma^2}{4} \frac{d}{dr} F(r), \\ X(r) &= 1 - \frac{\mu\sigma^2}{2\hbar^2} F(r). \end{aligned} \quad (38)$$

The first derivative term is eliminated by choosing $T(r) = \sqrt{X(r)}$ as then Eq. (37) becomes

$$\left[-\frac{\hbar^2}{2\mu} \nabla^2 + \frac{\Upsilon(r) - E}{X(r)} \right] \varphi(\mathbf{k}, \mathbf{r}) = 0, \quad (39)$$

so identifying

$$V(r, E) = E + \frac{\Upsilon(r) - E}{X(r)} \quad (40)$$

when

$$\begin{aligned}\Upsilon(r) &= J_0(r) - \frac{1}{r}J_1(r) - \frac{1}{2}\frac{d}{dr}J_1(r) - \frac{3}{2}\frac{1}{X(r)}J_1^2(r) \\ &= F(r) - \frac{\sigma^2}{8r}\frac{d}{dr}F(r) - \frac{\sigma^2}{16r}\frac{d^2}{dr^2}F(r) - \frac{3\mu\sigma^4}{32\hbar^2}\frac{1}{[1 - \mu\sigma^2/(2\hbar^2)]}F(r)\left[\frac{d}{dr}F(r)\right]^2\end{aligned}\quad (41)$$

Following Apagyi *et al.* [11], by considering local equivalent potentials at two energies E_1 and E_2 , it follows by using Eq. (40) that

$$\Upsilon(r) = \frac{E_2V(r, E_1) - E_1V(r, E_2)}{[V(r, E_1) - V(r, E_2) + E_2 - E_1]}, \quad (42)$$

and that

$$F(r) = \frac{\hbar^2}{\mu\sigma^2} \frac{2}{[V(r, E_1) - V(r, E_2) + E_2 - E_1]} \frac{V(r, E_1) - V(r, E_2)}{2}. \quad (43)$$

Then from Eqs. (38), one can find $J_0(r)$, $J_1(r)$, and $X(r)$, and so have a complete specification of the non-local interaction properties. To the extent that the energy dependent Frahn-Lemmer form describes p-¹²C scattering the functions, $U(r)$, $F(r)$ and $\Upsilon(r)$ should not be energy dependent. As will be seen, that is not completely the case with the system we have studied.

V. THE FRAHN-LEMMER POTENTIALS FOR $P - ^{12}\text{C}$

The central parts of the inversion potentials that were specified starting with phase shift sets from the g folding optical potential calculations of p-¹²C scattering at 100, 135, 160, and 200 MeV have been used in this study. With the non-locality range, σ , taken first as 0.7 and subsequently as 1.0 fm, the pairs of inversion potentials with energies 100 and 135 MeV, with 135 and 160 MeV, and with 160 and 200 MeV, have been used to find the functions $U(r)$, $F(r)$, and $\Upsilon(r)$ that characterize the non-local Frahn-Lemmer form of the p-¹²C optical potential. Results found using those pairs are identified by the notation 100-135, 135-160, and 160-200, and are portrayed in the next three figures by the solid, long dash, and short dash curves respectively. The real and imaginary parts of the various functions are given in the top and bottom sections of these figures with the results found using $\sigma = 0.7$ and 1.0 fm presented in the left and right side panels respectively.

The results for the local attribute $U(r)$ of the Frahn-Lemmer representations for the non-local optical potential are given in Fig. 4. In general those components are similar for all three energy pairs, and more so for the 135-160 and 160-200 cases. The variations in these results are but a few MeV in size. However there is a noticeable change in the degree of structure with marked oscillations in the results found with the smaller (0.7) non-locality range. Still the results with both non-locality range values do exhibit a residual energy dependence, and such is presumed not to be the case with the Frahn-Lemmer prescription. The modulating functions, $F(r)$, of the actual non-local term in the Frahn-Lemmer form are displayed in Fig 5. The real parts of this function are quite similar in the 135-160 and

160-200 cases although the overall strength of the real part of $F(r)$ decreases with the energy as it does with increase in the non-locality range. The 100-135 results (for the real part of $F(r)$) are larger than the others and varies from those in structure. The imaginary parts of $F(r)$ vary noticeably with the marked structure of the 100-135 results diminishing with energy. But the size change is not linear. Such energy dependence is also at odds with the Frahn-Lemmer requirement of an energy independent non-local potential. The local elements $\Upsilon(r)$ for these cases are shown in Fig. 6. They strongly reflect the properties of the relevant $F(r)$ albeit that the structures are enhanced.

In the next three figures the 100-135 and the 160-200 inversion potential pairs are shown again but now to compare more directly the effects of different choices of the non-locality range, σ . Results found with $\sigma = 0.7, 1.0,$ and 1.4 fm now are displayed by the solid, long dash, and short dash curves respectively. Again the real and imaginary parts of the characteristic functions $U(r), F(r),$ and $\Upsilon(r)$ are given in the top and bottom sectors of the diagrams. The $U(r)$ components are displayed in Fig. 7. The real parts for both energy pairs are similar with a decrease in the structure of the results being evident as the non-locality range increases. Indeed the results with $\sigma = 1.0$ and 1.4 fm are very similar. The imaginary parts of $U(r)$ have the form of an attractive well. Again the structure observed with the shortest range washes out when σ is increased. Now also the 160-200 MeV result changes strength noticeably with increase of the non-locality range. The results for $F(r)$ and $\Upsilon(r)$ are given in Figs. 8 and 9 respectively. The $\Upsilon(r)$ variations reflect those of $F(r)$ as before. In these cases changing the non-locality range has a dramatic effect, largely upon the magnitudes. In part though, that might be considered just an off-set to the normalization which depends on σ . But there are also changes in the structures. The disparity between the 100-135 and 160-200 results emphasizes again that there is a residual energy dependence one must consider if the set of fixed energy inversion potentials are recast as a Frahn-Lemmer type of non-local interaction.

VI. CONCLUSIONS

The fixed energy inverse scattering method of Lun *et al.* [5] has been used to specify local potentials from sets of phase shifts given by solutions of the Schrödinger equations with non-local optical potentials for proton- ^{12}C elastic scattering for a range of proton energies. Those (non-local potential) phase shift sets give very good fits to observed cross-section and analyzing power data [3]. So also then do the local (inversion) potentials as we have shown them to be both phase shift and observable equivalent (to the non-local potential expectations) to a high degree. As a non-local to local potential conversion scheme, the inverse scattering theory method has proved to be very effective. Irrespective of the pole term inherent in the inverse scattering theory method, the local inversion potentials do not resemble the simple functional forms, e.g. Woods-Saxon potentials, that are commonly used in phenomenological (numerical inversion) analyses of such scattering data.

We then considered a reverse mapping to see if and how the energy dependence of the inversion potentials might reflect a non-locality of simpler functional kind, and of the Frahn-Lemmer form in particular. The results are indicative of a characteristic forms for the diverse components of that simple non-local form of the interaction, but the detailed properties can vary significantly with the choice of the non-locality range, and there is an energy dependence

residual in the Frahn-Lemmer functions. Thus we contend that the energy dependence of local potentials for p- ^{12}C scattering (and by implication for other targets) whether those potentials are found by inversion or by phenomenology, is not solely a reflection of the true non-locality in the interaction between the nuclei. The non-locality itself is also energy dependent.

REFERENCES

- [1] K. Amos, P. J. Dortmans, S. Karataglidis, J. Raynal, and H. V. von Geramb, Adv. in Nucl. Phys. (2000) (in press); and references cited therein.
- [2] S. Karataglidis, P. J. Dortmans, K. Amos, and R. de Swiniarski, Phys. Rev. C **52**, 861 (1995); S. Karataglidis, B. A. Brown, P. J. Dortmans, and K. Amos, Phys. Rev. C **55**, 2826 (1997); P. J. Dortmans, K. Amos, and S. Karataglidis, J. Phys. G **23**, 183 (1997); Phys. Rev. C **55**, 2723 (1997); P. J. Dortmans, K. Amos, S. Karataglidis, and J. Raynal, Phys. Rev. C **58**, 2249 (1998).
- [3] P. K. Deb and K. Amos, Phys. Rev. C **62**, 016007 (2000).
- [4] H. Fiedeldey, R. Lipperheide, G. H. Rawitscher, and S. A. Sofianos, Phys. Rev. C **45**, 2885 (1992).
- [5] D. R. Lun, M. Eberspächer, K. Amos, W. Scheid, and S. J. Buckman. Phys. Rev. A **58**, 4993 (1998).
- [6] M.A. Hooshyar, J. Math. Phys. **16**, 257 (1975); *ibid* **19**, 253 (1978).
- [7] H. Huber and H. Leeb, Eur. Phys. J. **A1**, 221 (1998); J. Phys. **G24**, 1287 (1998).
- [8] H. Leeb, H. Huber, and H. Fiedeldey, Phys. Letts. **B344**, 18 (1995).
- [9] N. Alexander, K. Amos, B. Apagyi, and D. R. Lun, Phys. Rev. C **53**, 88 (1996).
- [10] R. Peierls and N. V. Mau, Nucl. Phys. **A343**, 1 (1980).
- [11] B. Apagyi, K-E. May, T. Häusser, and W. Scheid, J. Phys. G **16**, 451 (1990).
- [12] W. E. Frahn and R. H. Lemmer, Nuovo Cim. **5**, 523, 1564 (1957); F. Perey and B. Buck, Nucl. Phys. **32**, 353 (1962).
- [13] P. C. Sabatier, J. Math. Phys. **9**, 1241 (1968).
- [14] K. Chadán and P. C. Sabatier, *Inverse Problems in Quantum Scattering Theory*, 2nd Edition (Berlin, Springer, 1989).
- [15] M. Eberspächer, K. Amos, and B. Apagyi, Phys. Rev. C **61**, 64605 (2000).
- [16] K. E. May, M. Münchow, and W. Scheid, Phys. Lett. **141B**, 1 (1984).
- [17] J. Raynal, NEA 1209/05 (1999).

FIGURES

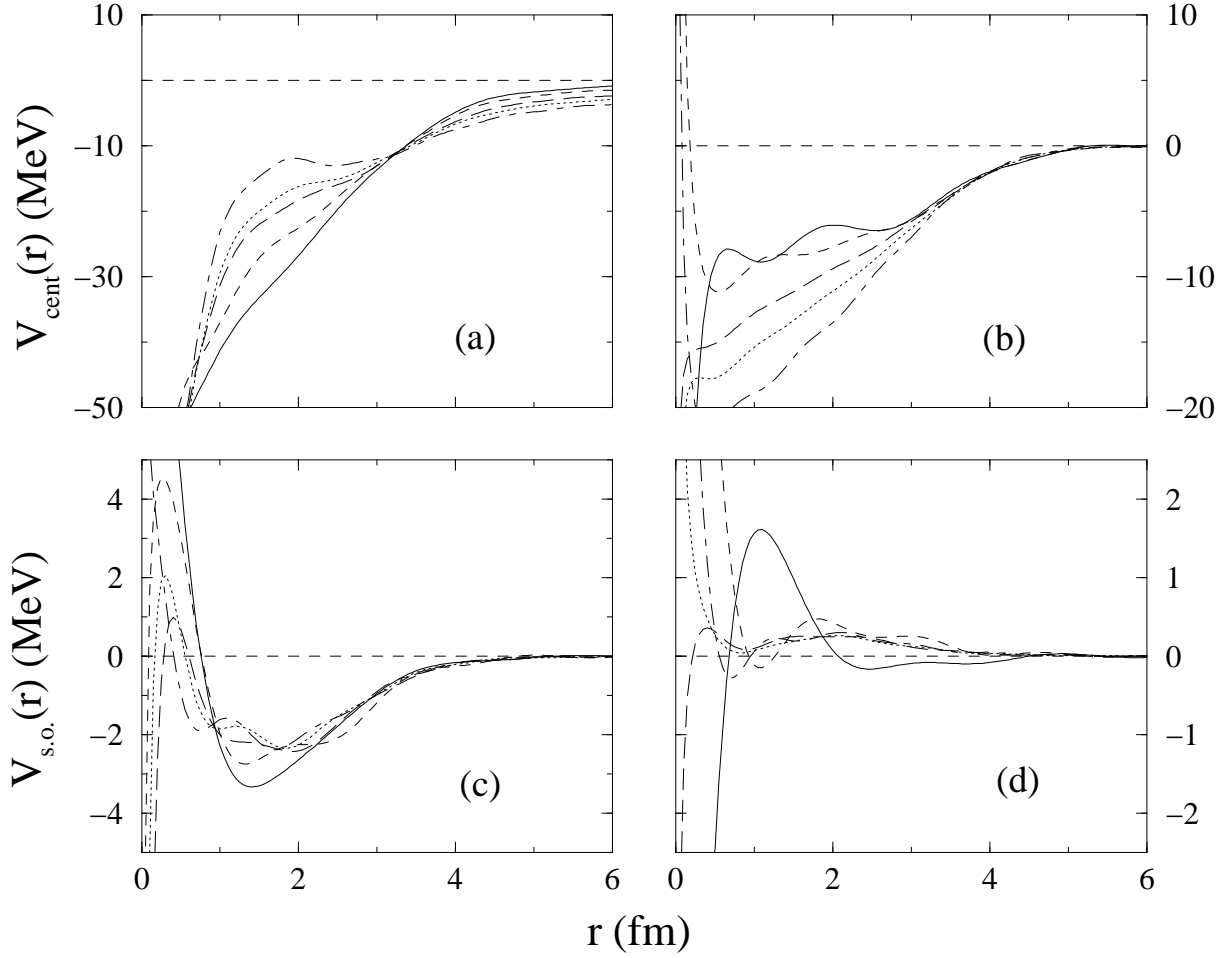


FIG. 1. Inversion potentials from p- ^{12}C scattering analyses portraying (a) the central real, (b) the central imaginary, (c) the spin-orbit real, and (d) the spin-orbit imaginary components. The separate energy results are identified in the text.

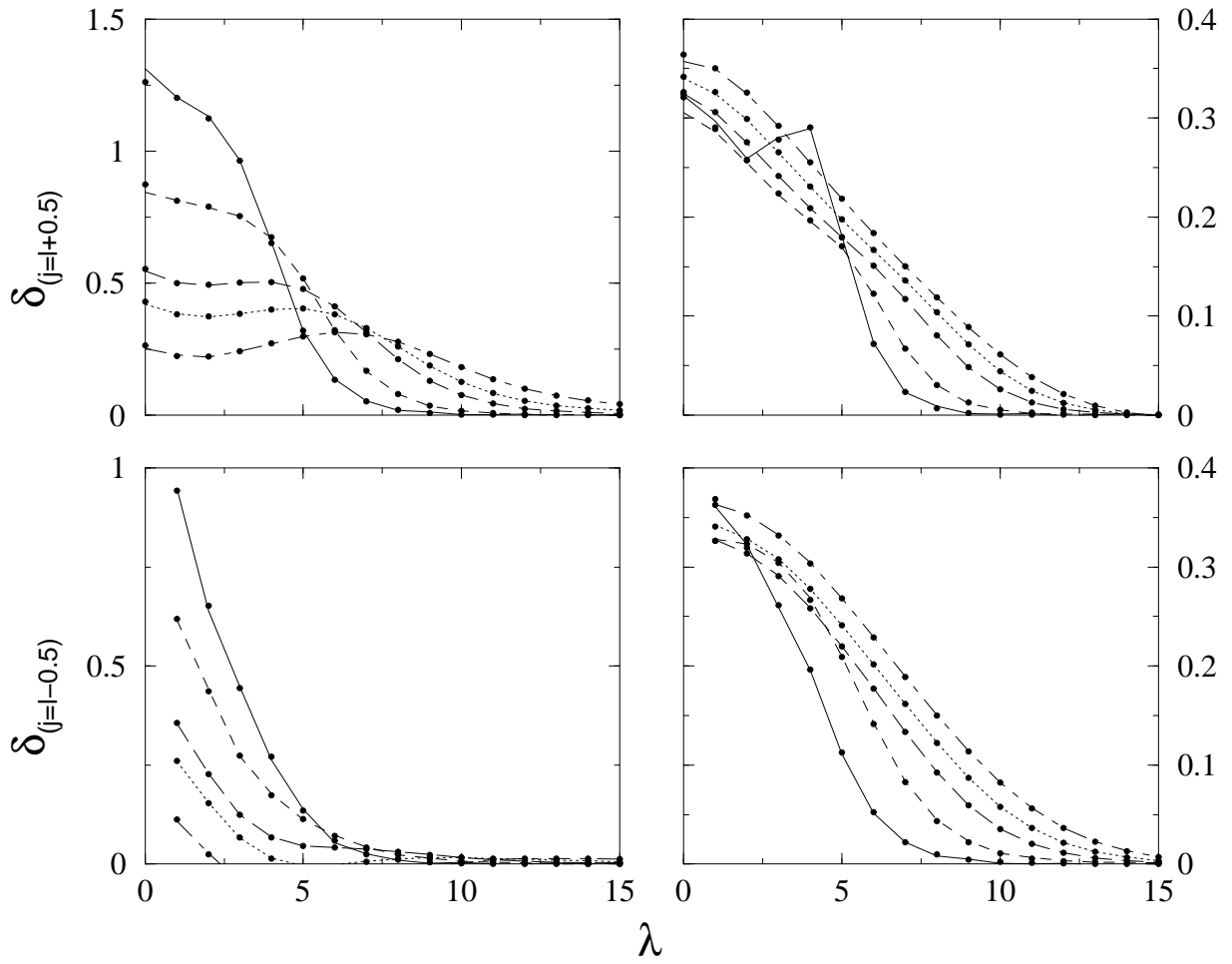


FIG. 2. The phase shifts in radians (real parts on the left, imaginary parts on the right) obtained using the inversion potentials given in Fig. 1 compared with the values used as input to the inversion procedure (filled dots). The lines connecting the physical values (integer l) identify the energies with the same scheme as used in Fig. 1.

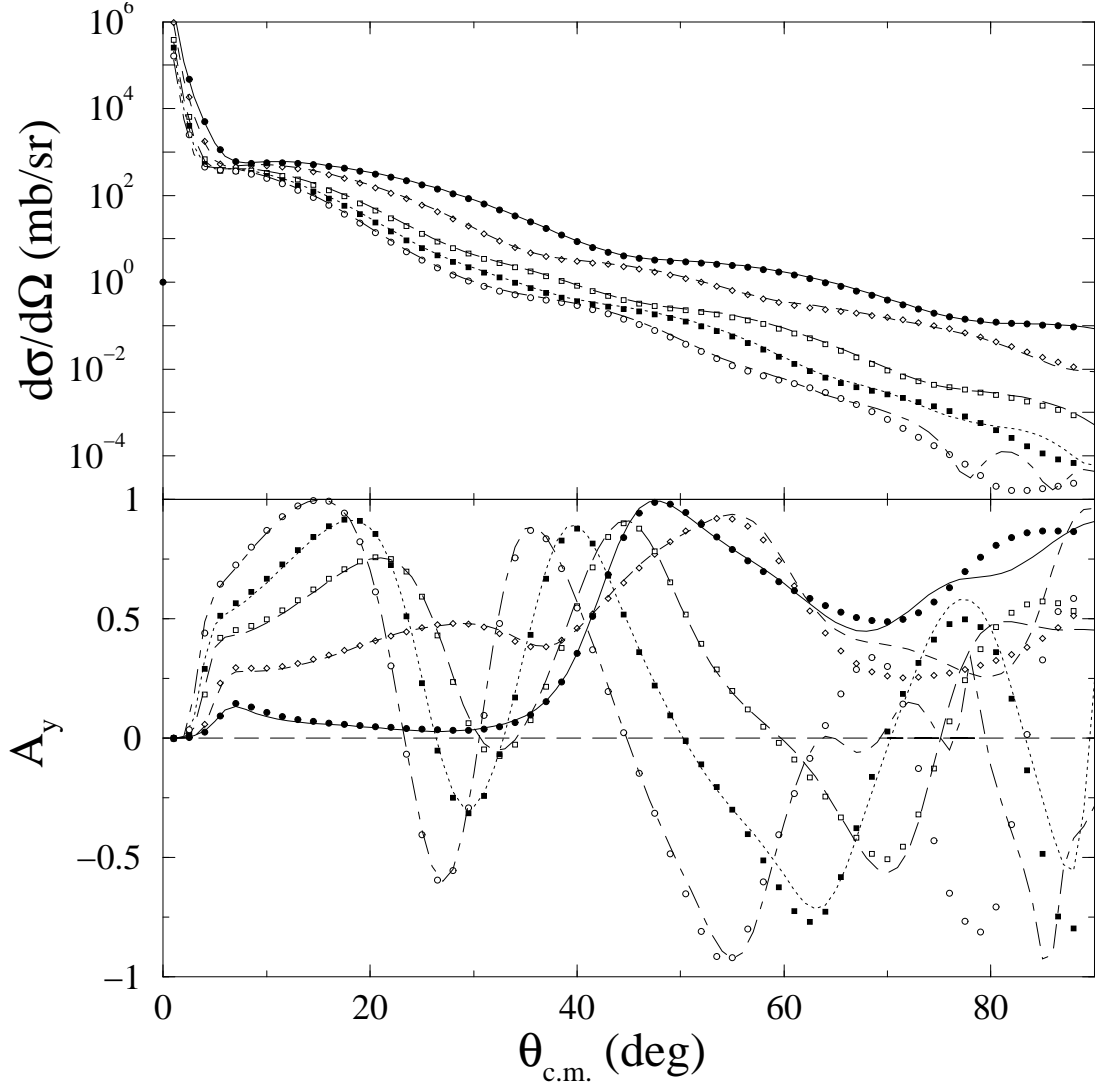


FIG. 3. The differential cross sections (top) and analyzing powers (bottom) obtained from use of the inversion potentials of Fig. 1 compared with the values associated with the phase shifts used as input to the inversion procedure. The lines indicate the disparate energy values as specified in the text as do diverse symbols for the ‘data’.

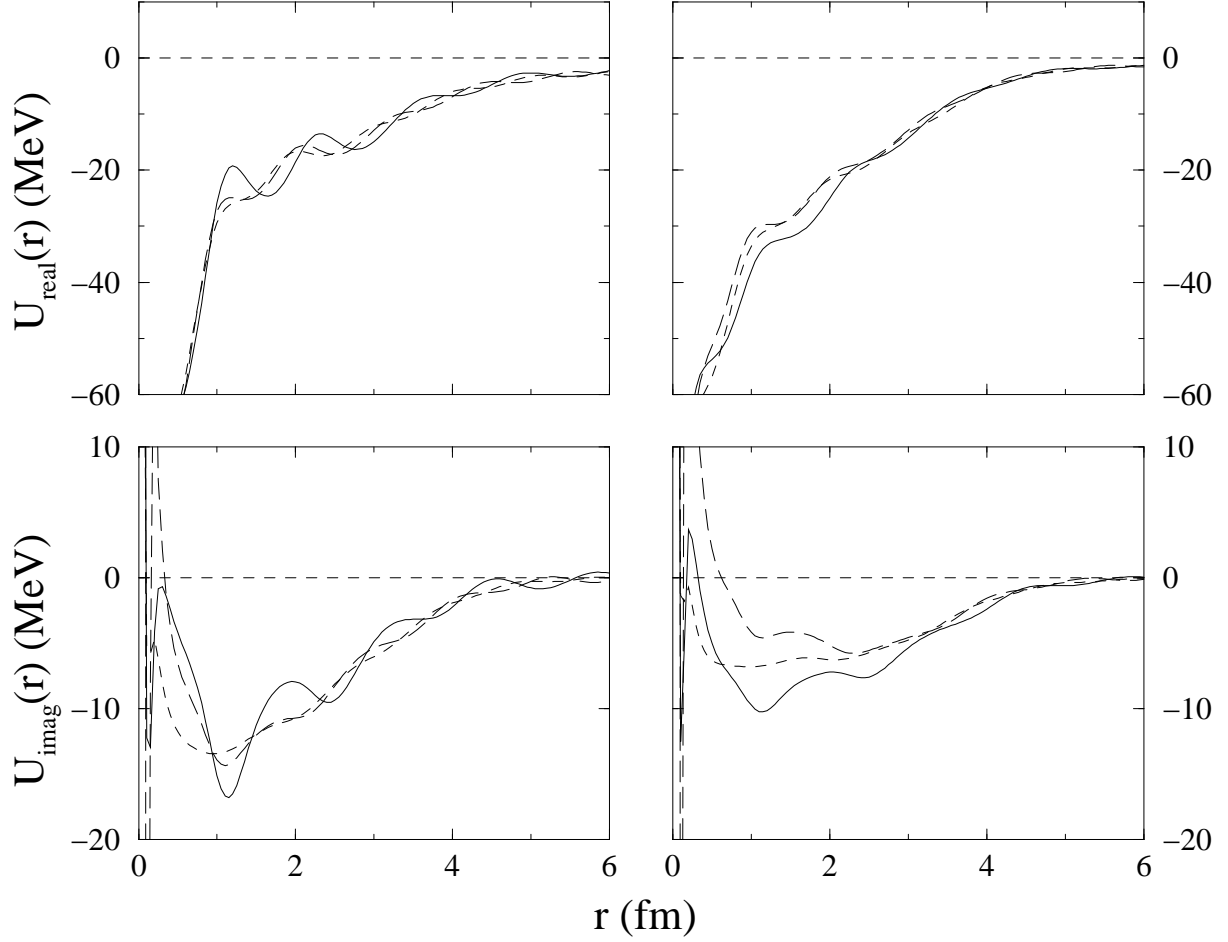


FIG. 4. The local components, $U(r)$ of Eq. (23), obtained with non-locality ranges, σ , of 0.7 and 1.0 fm (left and right panels respectively) and as deduced from the 100-135 MeV (solid curves), the 135-160 MeV (long dash curves), and the 160-200 MeV (short dash curves) pairs of (local) inversion potentials.

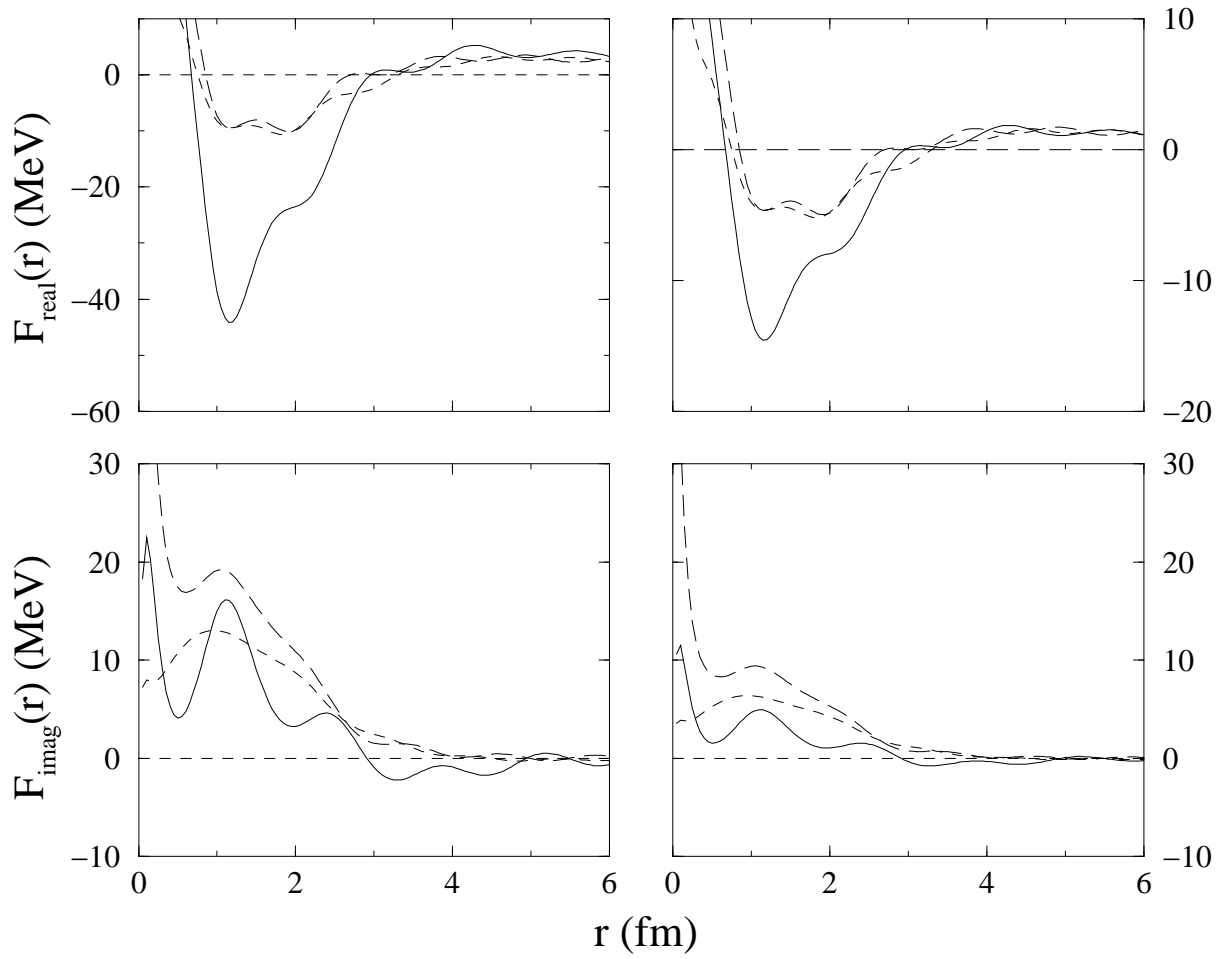


FIG. 5. As for Fig. 4, but for the non-local components, $F(r)$.

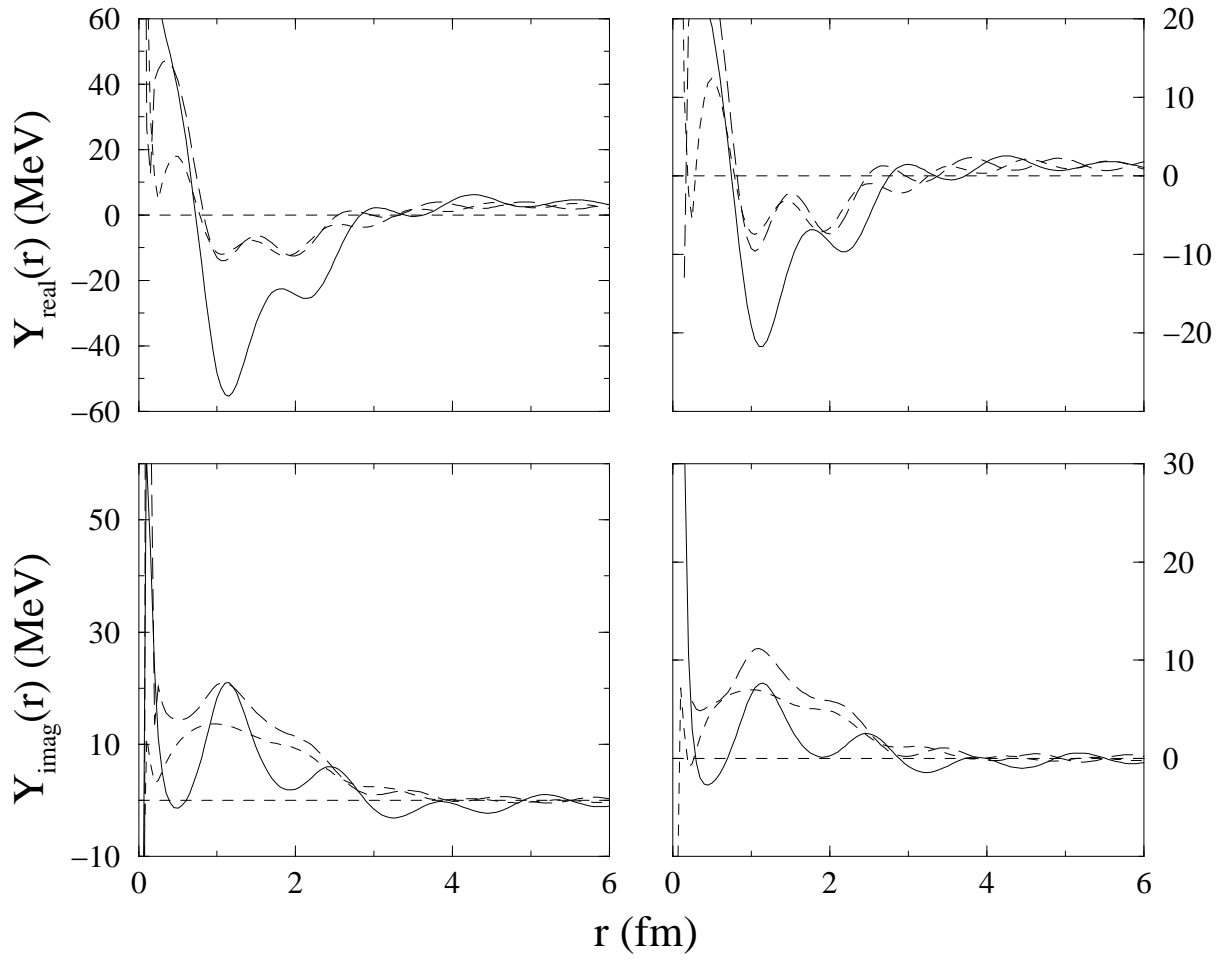


FIG. 6. As for Fig.4, but for the non-local components, $\Upsilon(r)$.

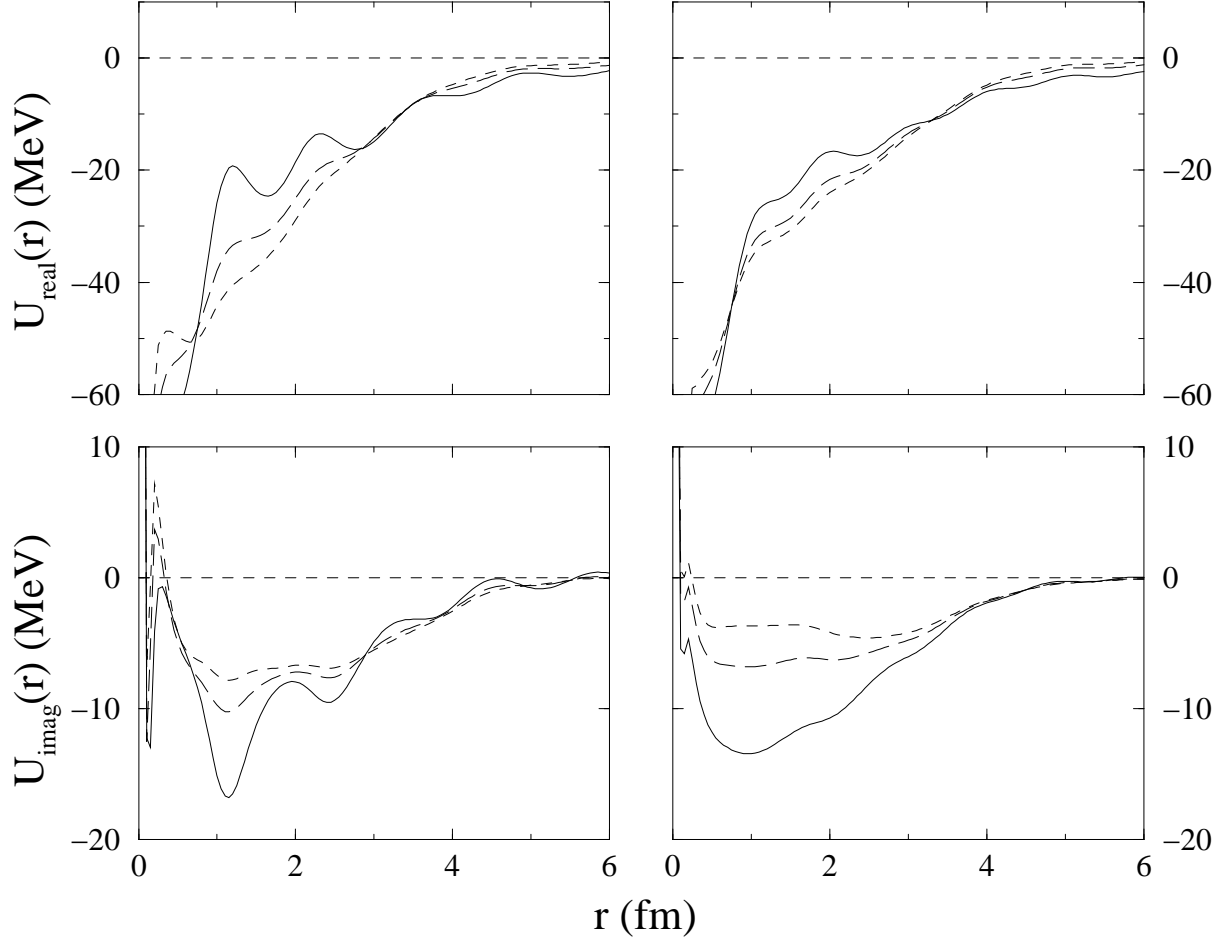


FIG. 7. The local terms $U(r)$ found using the 100-135 MeV (left) and the 160-200 MeV (right) pairs of inversion potentials but for Frahn-Lemmer non-locality ranges of 0.7, 1.0, and 1.4 fm. The results are portrayed by the solid, long dash, and short dash curves respectively.

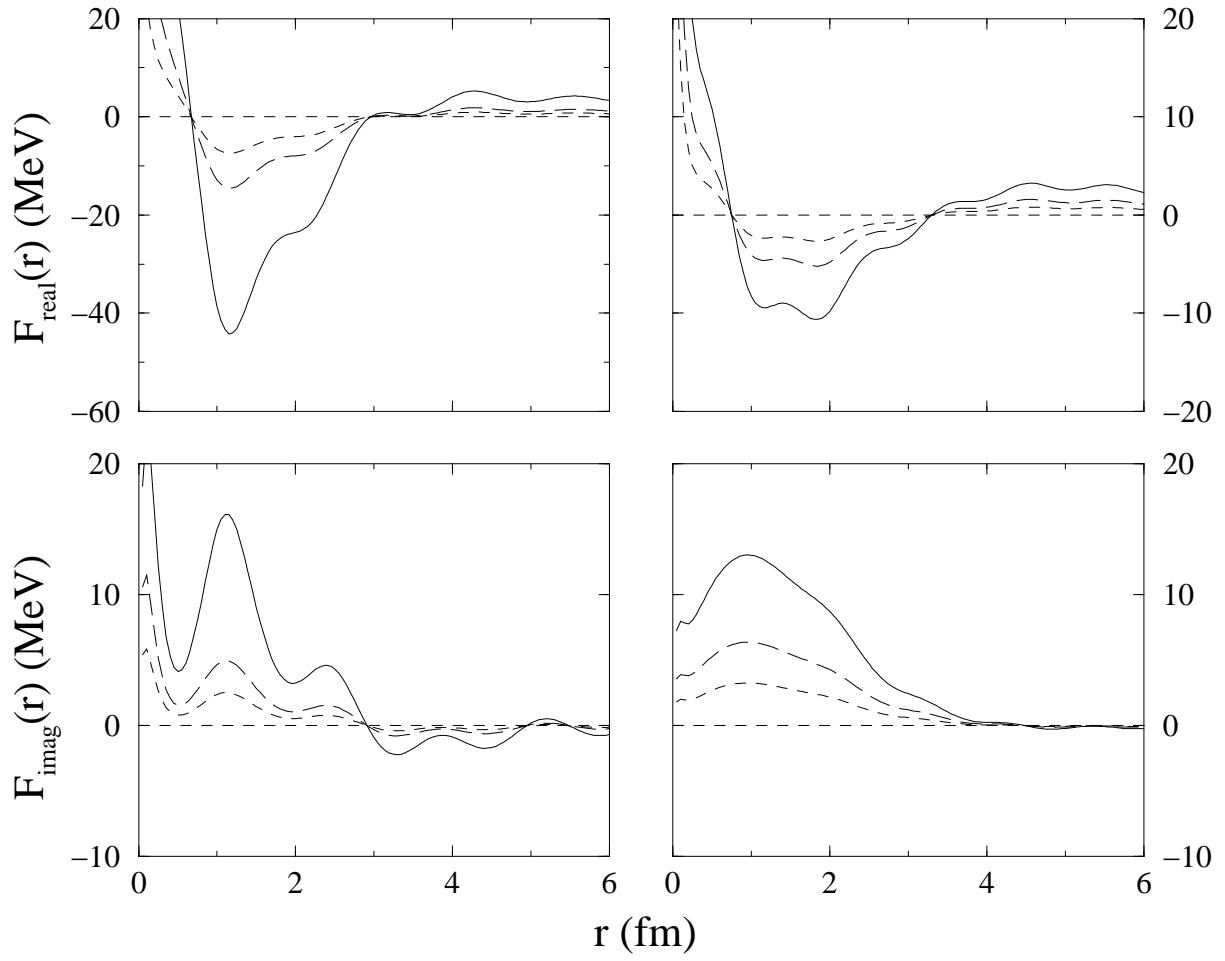


FIG. 8. As for Fig. 7, but for the non-local terms, $F(r)$.

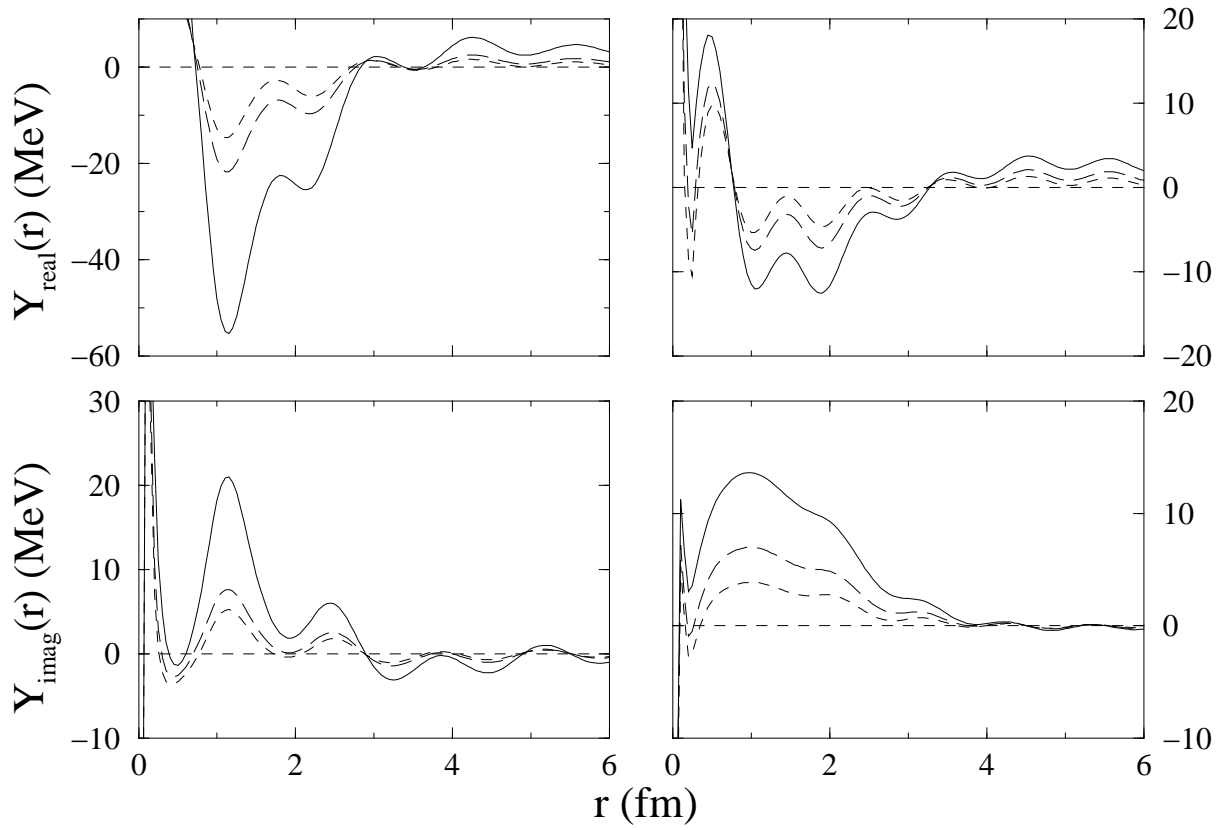


FIG. 9. As for Fig. 7, but for the non-local terms, $\Upsilon(r)$.